J. Membrane Biol. 178, 137–150 (2000)
DOI: 10.1007/s002320010021

The Journal of
Membrane
Biology

Ion Permeation and Selectivity of Wild-Type Recombinant Rat CNG (rOCNC1) Channels Expressed in HEK293 Cells

W. Qu[1], X.O. Zhu[1], A.J. Moorhouse[1], S. Bieri[2], A.M. Cunningham[2,3], P.H. Barry[1]
[1]School of Physiology and Pharmacology, The University of New South Wales, Sydney 2052, Australia
[2]Neurobiology Division, Garvan Institute of Medical Research, Darlinghurst, Sydney 2010, Australia
[3]School of Paediatrics, The University of New South Wales, Sydney 2052, Australia

Received: 3 July 2000/Revised: 29 August 2000

Abstract. The permeation properties of adenosine 3′, 5′-cyclic monophosphate (cAMP)-activated recombinant rat olfactory cyclic nucleotide-gated channels (rOCNC1) in human embryonic kidney (HEK 293) cells were investigated using inside-out excised membrane patches. The relative permeability of these rOCNC1 channels to monovalent alkali cations and organic cations was determined from measurements of the changes in reversal potential upon replacing sodium in the bathing solution with different test cations. The permeability ratio of Cl^- relative to Na^+ (P_{Cl}/P_{Na}) was about 0.14, confirming that these channels are mainly permeable to cations. The sequence of relative permeabilities of monovalent alkali metal ions in these channels was $P_{Na} \geq P_K > P_{Li} > P_{Cs} \geq P_{Rb}$, which closely corresponds to a high-strength field sequence as previously determined for native rat olfactory receptor neurons (ORNs). The permeability sequence for organic cations relative to sodium was $P_{NH3OH} > P_{NH4} > P_{Na} > P_{Tris} > P_{Choline} > P_{TEA}$, again in good agreement with previous permeability ratios obtained in native rat ORNs. Single-channel conductance sequences agreed surprisingly well with permeability sequences. These conductance measurements also indicated that, even in asymmetric bi-ionic cation solutions, the conductance was somewhat independent of current direction and dependent on the composition of both solutions. These results indicate that the permeability properties of rOCNC1 channels are similar to those of native rat CNG channels, and provide a suitable reference point for exploring the molecular basis of ion selectivity in recombinant rOCNC1 channels using site-directed mutagenesis.

Correspondence to: P.H. Barry

Key words: Recombinant rat cyclic nucleotide-gated channel (rOCNC1) — Selectivity — Permeation — Cation — Patch clamp

Introduction

Cation-selective cyclic nucleotide-gated (CNG) channels play central roles in mediating sensory signal transduction in olfactory receptor neurons (ORNs) and photoreceptors via the influx of monovalent and divalent cations (Getchell, 1977; Kurahashi & Shibuya, 1989; Zufall, Firestein & Shepherd, 1991, 1994). In ORNs, binding of odorants to their G-protein coupled receptors leads to an increase in cAMP, an activation of CNG channels and a subsequent influx of monovalent and divalent cations (Fesenko, Kolesnikov & Lyubarsky, 1985; Nakamura & Gold, 1987; Lancet & Ben-Arie, 1993). The cation permeability of these CNG channels has particular functional importance since the Ca^{2+} influx has further roles in the sensory transduction. It activates a Ca-dependent Cl^- channel to further depolarize the cell membrane (Kleene, 1993; Lowe & Gold, 1993) and provides some negative feedback by causing an inhibition of the activity of the CNG channels (Kramer & Siegelbaum, 1992; Balasubramanian, Lynch & Barry, 1996).

Although these CNG channels functionally belong to the class of ligand-gated channels, cloning and sequencing of several olfactory CNG channel subunits indicated that they share some similarity, especially in terms of transmembrane topology, to voltage-gated K^+ channels (Dhallan et al., 1990; Ludwig et al., 1990; Kaupp, 1995; Goulding et al., 1992). As in the K^+ channels, each subunit of the CNG channels contains six transmembrane-spanning segments and a pore-forming P region between TM5 and TM6. In addition, however,

the CNG channel subunits contain a cyclic nucleotide binding region near the C-terminus with a highly conserved hydrophobic ligand binding pocket (McKay & Steitz, 1981; Dhallan et al., 1990; Ludwig et al., 1990; Shabb & Corbin, 1992; Eismann, Bönigk & Kaupp, 1993).

While there is much structural homology between these two channel classes, the cation permeabilities of both channels are significantly different. Whereas the K^+ channels are highly selective for K^+ over Na^+ and divalent cations, the native CNG channels discriminate poorly amongst alkali and organic cations (e.g., Hille, 1975; Frings, Lynch & Lindemann, 1992; Balasubramanian, Lynch & Barry, 1995). The critical residues which confer such high K^+ selectivity in the K^+ channels are a glycine-tyrosine-glycine motif found within the P loop of all K^+ channels (Heginbotham, Abramson & MacKinnon, 1992). The fact that this motif is absent in the CNG channel subunits (Fig. 1*B*) undoubtedly contributes to the relative nonselectivity of CNG channels to the monovalent alkali ions. In fact, more recent structural information obtained from the related KcSA channel shows that the backbone carbonyl oxygen of these residues comprises the selectivity filter, forming binding sites for two permeating cations. In contrast, the molecular determinants of selectivity and permeation are much less understood for the CNG channels. In fact, previous measurements seemed to indicate that the CNG channels do not show significant anomalous mole fraction behavior (as tested with Na^+/Li^+ solutions; Frings et al., 1992), appearing to suggest that the pore of these channels may only contain a single ion occupancy site. Another residue, a glutamic acid (E363), situated adjacent to the G-Y-G motif (Fig. 1*B*), has been shown to be an important determinant of Ca^{2+} affinity in bovine rod CNG channels. Replacement of this residue with a neutral residue caused a marked decrease in the efficacy of Ca^{2+} block, while the mutation of the corresponding aspartate in the Shaker K^+ channel to a glutamate caused an increase efficacy of Ca^{2+} block of these channels (Root & Mackinnon, 1993; Eismann et al., 1994). Thus, while it is clear that these P loop residues contribute importantly to monovalent and divalent permeation, it is not yet clear exactly how this occurs and how the different CNG subunit sequences contribute to permeation in olfactory and other CNG channels. To begin to address these questions we report here a detailed characterisation of permeation in α-homomeric olfactory CNG channels.

Extensive biochemical experiments have demonstrated that CNG channels are tetrameric, consisting of α subunits (Kaupp et al., 1989; Ludwig et al., 1990; Weyand et al., 1994) and β subunits (Zagotta, 1996; Sautter et al., 1998; Gerstner et al., 2000). Studies of the rat olfactory CNG channel subunits recombinantly expressed in *Xenopus* oocytes or in a human embryonic kidney cell line (HEK 293) indicated that the α subunits themselves can form functional homomeric CNG channels (rOCNC1), but that the β subunit (rOCNC2) alone cannot produce any cAMP-activated currents. The properties of these α-homomeric rOCNC1 channels differ in a number of respects to both the native olfactory CNG channels and to the heteromeric rOCNC1/rOCNC2 channels. In particular the individual openings of the homomeric rOCNC1 channels are more prolonged and the channels show a 10-30-fold decrease in sensitivity to cAMP (Bradley et al., 1994). However it remains unclear exactly to what extent the α-subunits contribute to the permeation properties of the native olfactory CNG channels.

Consequently the aim of this paper is to make extensive and quantitative measurements on the characteristics of ion permeation of cAMP-activated rOCNC1 channels to address such issues. In particular, the selectivity of rOCNC1 channels to both alkali monovalent cations and monovalent organic cations was studied and the results compared with those obtained in native rat olfactory CNG channels and other cation-selective channels.

Materials and Methods

Transient Expression of rOCNC α1 Subunit cDNAs in HEK293 Cells

The cDNA encoding the α1 subunit of the rat olfactory cyclic-nucleotide-activated channel (rOCNC1; Dhallan et al., 1990; the kind gift of Dr. Randy Reed, Johns Hopkins University School of Medicine, Baltimore, MD) was first subcloned into a pCIS expression vector. Then the plasmid DNA was transiently transfected into exponentially growing human embryonic kidney (HEK) 293 cells using the calcium phosphate precipitation method of Chen & Okayama (1987). A second expression plasmid containing cDNA encoding the CD4 surface antigen was coexpressed into the same HEK293 cells, so that the surface of well-transfected cells could be labeled with CD4 antibody-coated polystyrene beads (Dynabeads M-450, Dynal A.S., Oslo, Norway). Only those transfected HEK 293 cells with sufficient beads 48–72 hr after transfection were chosen for experiments.

Electrophysiological Recording Procedure

Coverslips containing cultured transfected cells were transferred into the cell chamber (Fig. 1) and continuously buffered in General Mammalian Ringer's solution (GMR) which contained (in mM): 140 NaCl, 5 KCl, 2 $CaCl_2$, 1 $MgCl_2$, and 10 HEPES, titrated to pH 7.4 with 1 M NaOH. Cyclic AMP-activated currents were measured in voltage-clamp mode using inside-out patches (Hamill et al., 1981). For both macroscopic and single-channel current recordings, electrodes were pulled from borosilicate glass capillaries (Clark Electromedical Instruments, Reading, UK), and then fire-polished till the pipette resistance was 10–15 MΩ when filled with a Ca^{2+}-free control solution, which contained (in mM): 145 NaCl, 2 EGTA and 10 HEPES titrated to pH 7.4 with 1 M NaOH. To obtain clear single-channel recordings, pipettes with a smaller diameter than those used for macroscopic currents, and

cells expressing a lower density of bead labeling were chosen. During the experiments, the internal face of the patch was also perfused with this divalent cation-free control solution. Different test solutions were applied to inside-out patches in the test chamber using an array of eight parallel polyethylene tubes (Fig. 1). To examine the cation selectivity the 145 mM NaCl in the control solution was replaced by 145 mM of the chloride salt of the test cation. To examine the cation/anion permeability of the channels, the 145 mM NaCl in the control solution was replaced by each of two NaCl dilutions: one with a composition (in mM) of: 75 NaCl, 2 EGTA, 10 HEPES and 136 sucrose, and the other (in mM): 37.5 NaCl, 2 EGTA, 10 HEPES and 189 sucrose. All the test solutions were titrated to pH 7.4 with 1 M Tris-base, except hydroxylamine, which was titrated to pH 5.8 in order to increase the ionized fraction of the permeating ion.

Currents were recorded and voltage protocols were applied using an Axopatch-1D amplifier (Axon Instruments, Foster City, CA) via a Digidata 1200 A/D converter controlled by a 166 MHz Pentium computer running pCLAMP 8.0 software (Axon Instruments, Foster City, CA). Data were low-pass filtered with a cutoff frequency of 2 kHz (4-pole Bessel filter) and digitized at 5 kHz. Single-channel conductances were measured either by fitting Gaussian distributions to amplitude histograms (15-sec recordings) or by manually determining the mean peak current at each membrane potential (1.5-sec pulse recordings). The open probability was measured from 15-sec long recordings by constructing open and closed event lists using a threshold set to 50% of the amplitude of the main conductance level (Fetchan 6.0). Typically only 1-3 channels were present in the patches used for these recordings and values of open probabilities given for different solutions were all measured in the same patch, and where there were more than 1 channel in the patch, the open probability was appropriately corrected. Experiments were performed at room temperature (20 ± 2°C). Liquid junction potentials were calculated for each solution using the MS Windows version of the software program JPCalc (Barry, 1994; with additional mobility values from Ng & Barry, 1995 and an unpublished observation of David Tridgell for the mobility of hydroxylamine). Averaged data are given as mean ± SEM. Differences between mean values were analyzed using either an analysis of variance, when comparing multiple values, or the Student's paired *t*-test for paired experiments.

Reversal Potentials and Permeability Ratios

Reversal potentials (E_{rev}) were determined from fitting regression lines to current-voltage curves. The values of E_{rev} obtained were then fitted to the Goldman-Hodgkin-Katz (GHK) voltage equation (e.g., Hille, 1992), taking into account the permeability of the channels to $Tris^+$ (used in all solutions to adjust pH). The relative permeability of chloride to sodium ions (P_{Cl}/P_{Na}) was thus given by the following equation:

$$E_{rev} = (RT/F)\ln\{([Na^+]_o P_{Tris}/P_{Na}\,[Tris^+]_o + P_{Cl}/P_{Na}\,[Cl^-]_i)\,/\,([Na^+]_i + P_{Tris}/P_{Na}\,[Tris^+]_i + P_{Cl}/P_{Na}\,[Cl^-]_o)\} \quad (1)$$

where R, T and F have their usual meaning and $[Cl^-]_i$, $[Na^+]_i$, $[Tris]_i$; $[Cl^-]_o$, $[Na^+]_o$ and $[Tris]_o$ are the activities of Cl^-, Na^+ and of $Tris^+$ in the intracellular and extracellular solutions, respectively, and P_{Cl}/P_{Na} and P_{Tris}/P_{Na} are the permeabilities of Cl^- and of $Tris^+$, relative to the Na^+ permeability. Permeability ratios for test cations X^+ relative to Na^+ (P_X/P_{Na}) were calculated using the following modified GHK voltage equation (*see* appendix in Balasubramanian et al., 1995):

$$(P_X/P_{Na})^* = ([Na^+]_i/[X^+]_i)\exp(-F\Delta E_{rev}/RT) \quad (2)$$

where $(P_X/P_{Na})^*$ represents the apparent X^+ to Na^+ permeability ratio, $[X^+]_i$ and $[Na^+]_i$ are the activities of test cation X^+ and Na^+ in the intracellular test solutions, and ΔE_{rev} the change in the reversal potential when the NaCl control solution was replaced by the test solution (X^+ relative to Na^+). In addition, Eq. (2) makes the assumption that P_{Cl} is very small and for a first approximation that P_{Tris} can be ignored. In the above calculations, activities were approximated by concentrations, since the ionic strength of the solutions remained fairly constant. To correct for the permeability of $Tris^+$, the following equation was used to determine the corrected permeability ratio (P_X/P_{Na}; Appendix in Balasubramanian et al., 1995):

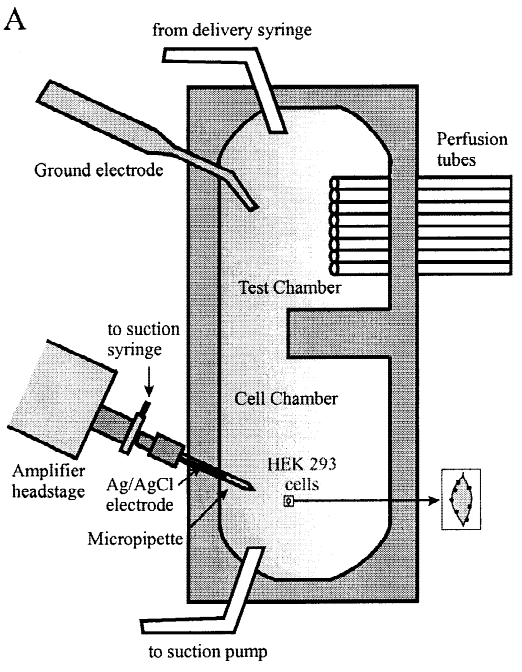

B

PUTATIVE PORE (P loop)

Shaker B K^+ Channel	418	P	D	A	F	W	W	A	V	V	T	M	T	T	V	G	Y	G	D	M	T	P	V	G	440
Bovine Rod Channel	348	V	Y	S	L	Y	W	S	T	L	T	L	T	T	I	G	-	-	E	T	P	P	P	V	368
rOCNC1 channel	327	I	Y	C	L	Y	W	S	T	L	T	L	T	T	I	G	-	-	E	T	P	P	P	V	347
rOCNC2 channel	219	L	Y	S	F	Y	F	S	T	L	I	L	T	T	V	G	-	-	D	T	P	L	P	D	239

Fig. 1. (*A*) The patch-clamp recording setup (adapted from Fig. 1 of Balasubramanian et al., 1996). Micropipettes were assembled onto the Ag/AgCl electrode that was connected to the amplifier headstage. The headstage and the pipette holder assembly were fixed right above the microscope stage at an angle of about 45°. Coverslips containing cultured transfected HEK293 cells were placed in the cell chamber and bathed in the continuously flowing GMR solution. The ground electrode was placed in the test chamber to minimize noise interference. After formation of an inside-out patch, the pipette, along with the attached patch, was moved to the test chamber, right in front of a set of perfusion tubes, which were used to apply the various test solutions. (*B*) Aligned amino acid sequences for comparison from the putative pore region of the Shaker B K^+ channel, bovine rod CNG channel, rOCNC1 and rOCNC2 protein channels. In the alignment, a dash indicates the absence of an amino acid.

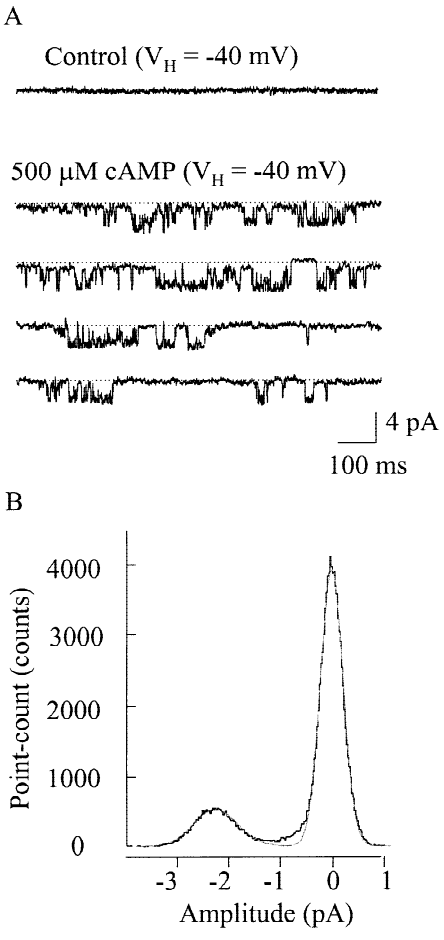

Fig. 2. Single-channel properties of cAMP-activated currents of rOCNC1 channels expressed in HEK 293 cells. (*A*) Representative single-channel currents elicited by 500 μM cAMP in an inside-out membrane patch. The holding potential (V_H), measured as V_P, was −40 mV; sampling frequency, 1 kHz and low-pass filter frequency, 500 Hz. The dashed lines indicate the closed state. (*B*) All-point amplitude histogram of current for the single-channel records illustrated in (*A*). The continuous curve represents a double Gaussian distribution. The peak of the first Gaussian was close to zero and corresponded well to the control histogram obtained in the absence of cAMP at the same membrane potential. The peak of the second Gaussian, corresponding to the mean amplitude of the single-channel currents, was about −2.3 pA.

$$(P_X/P_{Na}) = [(P_X/P_{Na})^* \times (1 + \beta_2)] - \beta_1 \quad (3)$$

where $\beta_2 = (P_{Tris}/P_{Na}) \times ([Tris^+]_i^{Na}/[Na^+]_i)$ and $\beta_1 = (P_{Tris}/P_{Na}) \times ([Tris^+]_i^{X}/[X^+]_i)$. Superscripts ^{Na} and ^{X} indicate that the Tris concentration refers to the values in the Na and X solutions, respectively.

Results

General Properties of Single cAMP-Activated Currents

In divalent cation-free symmetrical NaCl solutions, inside-out membrane patches excised from HEK293 cells showed no channel openings at a membrane potential of −40 mV (Fig. 2*A*). When the excised patches were held at a membrane potential of −40 mV and the cytoplasmic side was exposed to a saturating concentration of cAMP (500 μM), inward currents ranging from fluctuations of a few pA ("single channel currents") to about 50 pA ("macroscopic currents") were observed, reflecting the different numbers of CNG channels in the patches. Figure 2*A* shows single channel current fluctuations during a prolonged exposure to cAMP. As previously reported (e.g., Bradley et al., 1994), single α-homomeric rOCNC1 channels opened for prolonged bursts, which were interrupted by brief closures, and failed to show any significant desensitization during continuous cAMP exposure. In 5 patches containing only a few channels, the mean open probability of the channel during a 15-sec exposure to 500 μM cAMP at a membrane potential of +40 mV was approximately 33 ± 16% with a maximum open probability of about 80%. These are somewhat lower values than those reported by Bönigk et al. (1999) for similar recombinant CNG channels. However, there was significant variability in open probability from patch-to-patch (*see also* Table 2 of Li & Lester, 1999). As illustrated in Fig. 2*B*, the single channel amplitude was resolved with the use of Gaussian fits to all-point amplitude histograms. At a membrane potential of +40 mV, the mean amplitude of rOCNC1 single-channel currents induced by 0.5 mM cAMP was −1.8 ± 1.0 pA ($n = 5$), corresponding to an averaged single channel chord conductance (γ) of 45.5 ± 19.9 pS ($n = 5$, range: 25–75 pS), assuming a reversal potential in symmetrical NaCl solutions of 0 mV. To compare the properties of multiply activated channels with those of single channels, the following macroscopic and single channel currents were analyzed separately.

Relative Permeability Ratios of Na^+ and Cl^-

The chloride-to-sodium permeability ratio (P_{Na}/P_{Cl}) in rOCNC1 channels was measured by perfusing the internal side of the membrane with three different bath solutions containing 145 mM, 75 mM and 37.5 mM NaCl while the pipette solution (145 mM NaCl) was kept constant. Currents were elicited by applying 1.5 sec test pulses from −80 to +80 mV in 20 mV increments in the presence of 500 μM cAMP. Representative macroscopic and single-channel currents are shown in Fig. 3*A–C* and Fig. 4*A–C*.

The *I–V* relations of both macroscopic and single-channel current recordings showed a positive shift in E_{rev} with a decrease in $[Na^+]_i$ (Fig. 3 *a–c* and 4 *a–c*). The mean E_{rev} values from single-channel currents, corrected for liquid junction potentials, were: 0.3 ± 0.4 mV in 145 mM NaCl ($n = 7$), 10.5 ± 1.0 mV in 75 mM NaCl ($n =$

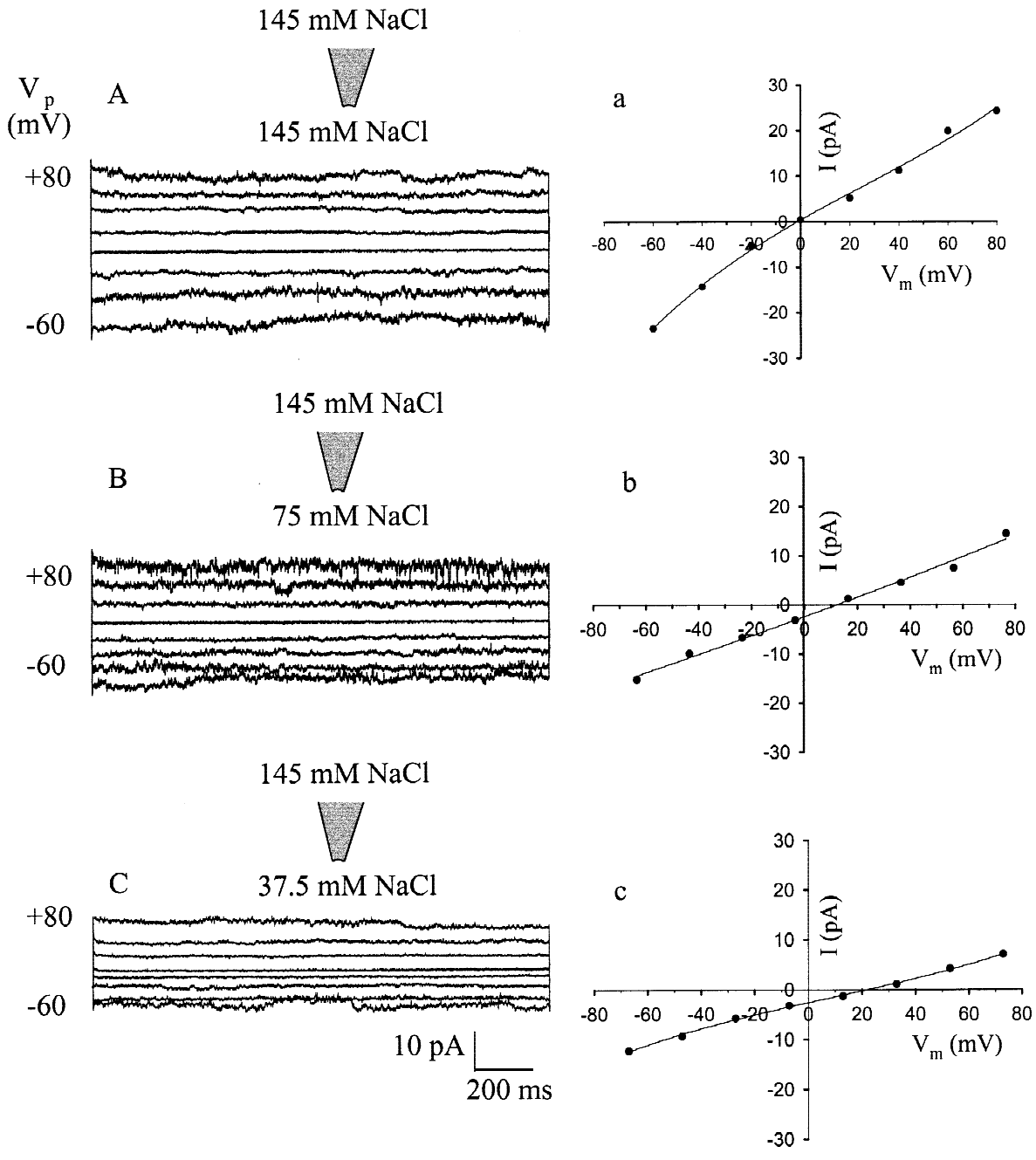

Fig. 3. Macroscopic cAMP-activated currents obtained in different NaCl dilutions. (*A*), (*B*) and (*C*) are representative macroscopic currents through rOCNC1 channels in one inside-out patch where the intracellular NaCl concentration was changed and the extracellular (pipette) NaCl (145 mM) one was kept constant. Currents were activated by 500 μM cAMP in response to 1.5-sec voltage pulses (shown as V_P) from −60 mV to +80 mV in 20-mV steps. The holding potential was 0 mV and background current traces in the absence of cAMP have been subtracted. (*a*), (*b*) and (*c*) are the corresponding current-voltage (*I–V*) relations for each set of traces. E_{rev} for each solution in this same patch was close to the equilibrium potentials of Na^+, which were about −1 mV for 145 mM NaCl, +12 mV for 75 mM NaCl and +20 mV for 37.5 mM NaCl, respectively. Note that the trace voltages are given as pipette potentials (V_P) and the fully corrected voltages are shown in the *I–V* plots as the membrane potentials (V_m) in this and in subsequent figures.

4) and 23.7 ± 1.7 mV in 37.5 mM NaCl ($n = 6$), respectively. The E_{rev} values obtained from macroscopic and single-channel currents were not significantly different ($P > 0.05$). P_{Cl}/P_{Na} was then obtained by fitting E_{rev} to the modified GHK equation (Eq. 1). Figure 5 plots the mean reversal potential of cAMP-induced currents against internal sodium activities (using mean activity coefficients, obtained from Robinson & Stokes, 1965).

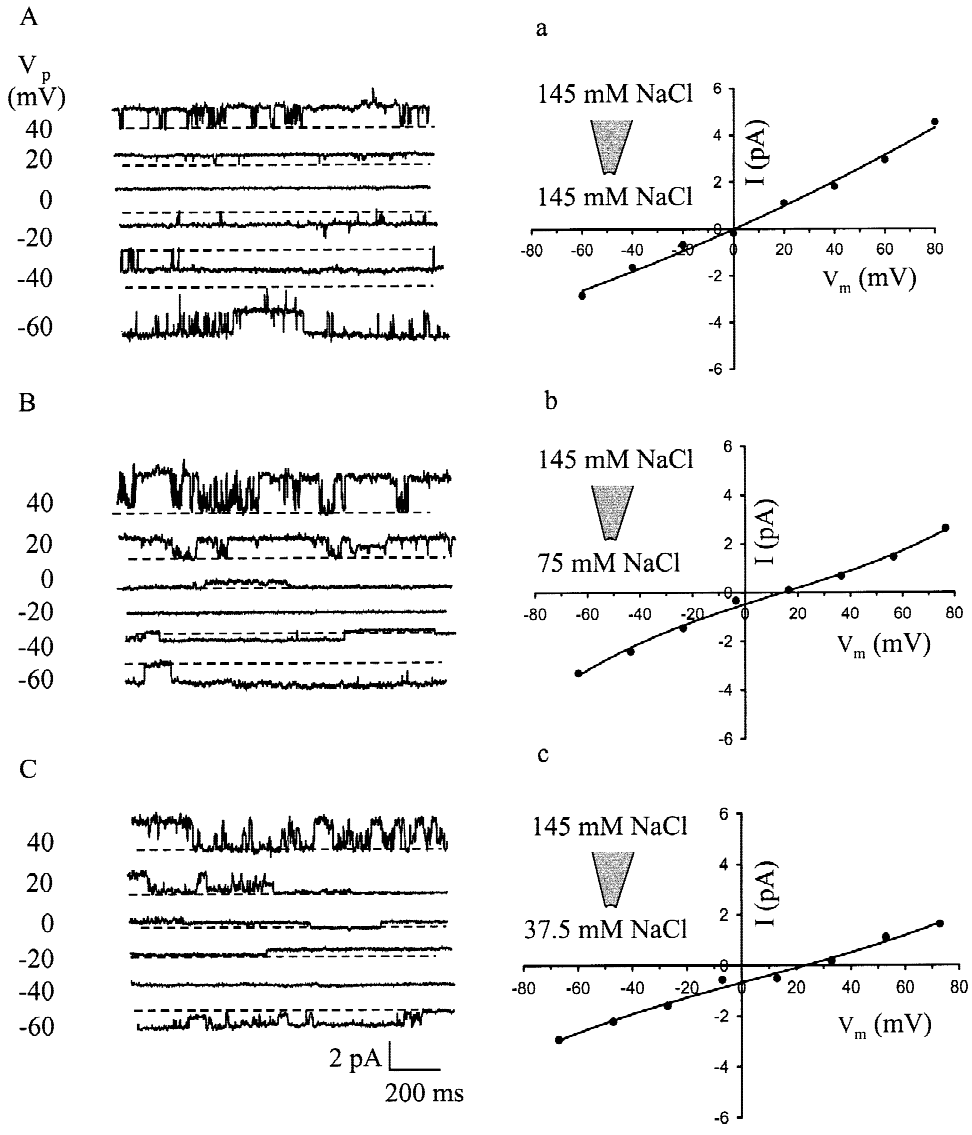

Fig. 4. Single-channel cAMP-activated currents obtained in different NaCl dilutions. (*A*), (*B*) and (*C*) are the representative single-channel current records at different holding potentials (V_P) recorded in 145, 75 and 37.5 mM intracellular NaCl. Closed states are marked with broken lines. (*a*), (*b*) and (*c*) are the current-voltage curves of the main open state for each of the traces. E_{rev} values for each solution, measured as V_m for the same patch, were about 0 mV for 145 mM NaCl, +15 mV for 75 NaCl and +23 mV for 37.5 NaCl, respectively.

The dashed line for an ideal cation selective channel was obtained from Eq. (1) with $P_{Cl}/P_{Na} \approx 0$. It can be clearly seen that the reversal potentials deviated from the behavior of an ideally cation-selective channel, with the best fit to the data to the GHK equation (Eq. 1) giving a relative permeability ratio, P_{Cl}/P_{Na}, = 0.14. Similar deviations from ideal cation selectivity were reported for native CNG channels of rat ORNs (Balasubramanian et al., 1995) and for the native CNG channels from rat rods (Zimmerman & Baylor, 1992). The open probability did not seem to be markedly affected by the concentration of the permeant ion. For example, for the patch illustrated in Fig. 4*A–C*, the open probability at the membrane potential of +40 mV was 56, 67 and 52% in 145, 75 and 37.5 mM NaCl solutions, respectively. The results indicated that, although the cyclic AMP-activated rOCNC1 channel is predominantly permeable to Na^+, it does have a small but significant permeability to Cl^-.

Selectivity for Different Monovalent Alkali Cations

The cation selectivity of the cyclic AMP-activated rOCNC1 channel under these divalent cation-free condi-

tions was characterized by sequentially perfusing solutions containing different equimolar alkali metal cations to the intracellular side of excised patches. Both macroscopic and single-channel currents were measured. Figure 6*A–E* shows representative macroscopic current traces from one patch in the presence of different test solutions. The mean reversal potentials (E_{rev}), obtained from fits of quadratic polynomials to the *I–V* curves and corrected for junction potentials under each ionic condition (e.g., Fig. 6*a–e*), were: −0.3 ± 0.2 mV for Na^+ ($n = 3$), 0.7 ± 0.5 mV for K^+ ($n = 3$), 8.2 ± 1.4 mV for Li^+ ($n = 3$), 12.8 ± 1.9 mV for Cs^+ ($n = 3$) and 15.1 ± 2.3 mV for Rb^+ ($n = 3$). Similar results were also obtained from single-channel recordings (Fig. 7*A–E*) with the mean values of E_{rev} under each ionic condition (e.g., Fig. 7*a–e*) being: 0.2 ± 0.3 mV for Na^+ ($n = 7$), 1.6 ± 1.5 mV for K^+ ($n = 6$), 7.2 ± 2.2 mV for Li^+ ($n = 5$), 12.8 ± 1.6 mV for Cs^+ ($n = 5$) and 14.9 ± 2.0 mV for Rb^+ ($n = 6$). There were no significant differences between these reversal potential values obtained from the macroscopic and single-channel currents. At a membrane potential of +40 mV, the open probabilities of single-channel currents obtained in rOCNC1 channels were 67 ± 6% for Li^+ ($n = 3$), 50 ± 18% for Na^+ ($n = 3$), 52 ± 23% for K^+ ($n = 3$), 51 ± 25% for Rb^+ ($n = 3$) and 43 ± 7% for Cs^+ ($n = 3$), respectively. These values were not significantly different from each other ($P > 0.05$), therefore providing no evidence that the nature of the permeating ion affected channel gating.

The values of E_{rev} obtained from single-channel recordings were then used to calculate the permeabilities of these alkali cations relative to sodium using the modified GHK equation (Eq. 2), having corrected for $Tris^+$ permeability (Eq. 3). The results were as follows: P_{Na} (1) ≥ P_K (0.97) > P_{Li} (0.77) > P_{Cs} (0.62) ≥ P_{Rb} (0.57). The ionic selectivity of rOCNC1 channels was further investigated by measuring the single-channel conductance in different solutions at −80 and +80 mV (Table 1). For example, at the membrane potential of +80 mV, the single channel conductance ratios, relative to sodium and obtained in the different solutions in three patches were: g_{Na} (1) > g_K (0.92 ± 0.02) > g_{Li} (0.65 ± 0.07) > g_{Cs} (0.42 ± 0.05) > g_{Rb} (0.25 ± 0.04). Figure 8 illustrates a plot of these conductance ratios at the membrane potential of +80 mV against the ionic radius of the test cations. At a membrane potential of +80 mV, both conductivity and permeability data showed that the rOCNC1 channels were approximately equally permeable to Na^+ and K^+, less permeable to Li^+ and markedly less permeable to Cs^+ and Rb^+ (Table 1).

Thus, the cation permeability sequence for alkali monovalent cations through the rOCNC1 channels was: $P_{Na+} \geq P_{K+} > P_{Li+} > P_{Cs+} \geq P_{Rb+}$, and the conductance sequence at +80 mV was: $\gamma_{Na+} \geq \gamma_{K+} > \gamma_{Li+} > \gamma_{Cs+} > \gamma_{Rb+}$.

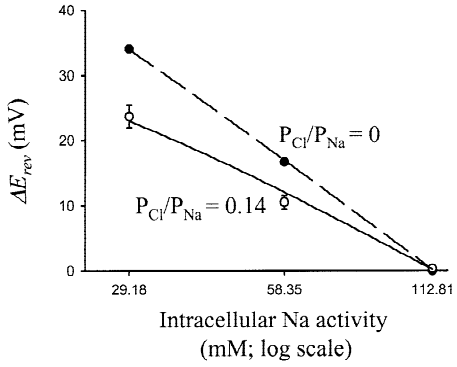

Fig. 5. The relative permeability ratio, P_{Cl}/P_{Na}, for rOCNC1 channels. P_{Cl}/P_{Na} was determined by plotting the averaged E_{rev} under different internal NaCl concentrations against the *activities* of intracellular Na^+ (on a log scale). The best-fit continuous line was obtained by fitting data points to the GHK equation (Eq. 1) with $P_{Cl}/P_{Na} = 0.14$ and corrected for P_{Tris}/P_{Na}. The dashed line represents the perfectly selective channel with $P_{Cl}/P_{Na} = 0$.

Permeability of cAMP-Activated rOCNC1 Channels to Organic Cations

The selectivity of the cAMP-activated rOCNC1 channels in HEK293 cells to organic cations was similarly investigated in single-channel recordings in inside-out patches. Na^+ on the cytoplasmic side of the patch was replaced by equimolar concentrations of different organic cations (145 mM) in all cases, except hydroxylammonium$^+$ ($OHNH_3^+$), which was calculated as 65 mM at pH 5.8. Although it is possible that the different pH may change the pore and/or gating properties of these rOCNC1 channels which would complicate the interpretation of the results obtained with hydroxylammonium, there did not seem to be much divergence from the predicted permeability ratio or even marked effects on channel open probability. Figure 9*A–E* shows the representative single-channel currents in the presence of ammonium$^+$ (NH_4^+) and hydroxylammonium$^+$ ($OHNH_3^+$), tetraethylammonium$^+$ (TEA^+), choline$^+$ and (hydroxymethyl) aminomethane$^+$ ($Tris^+$) in one patch. Clearly it can be seen that rOCNC1 channels, as with native rat olfactory CNG channels, are appreciably permeable to all the test organic cations, including those, such as TEA^+, with large molecular weights (mol. wt. 130.7; Picco & Menini, 1993; Balasubramanian et al., 1995). At a membrane potential of +60 mV, the open probabilities of single-channel currents obtained in each organic cation solution were respectively 41 ± 16% for NH_4^+ ($n = 3$), 28 ± 5% for $OHNH_3^+$ ($n = 3$), 29 ± 5% for Na^+ ($n = 3$), 27 ± 5% for choline$^+$ ($n = 3$), 43 ± 11% for $Tris^+$ ($n = 3$) and 39 ± 10% for TEA^+ ($n = 3$). These results were not significantly different from each other ($P > 0.05$), indicating that the channel gating was not significantly altered by the presence of various organic cations.

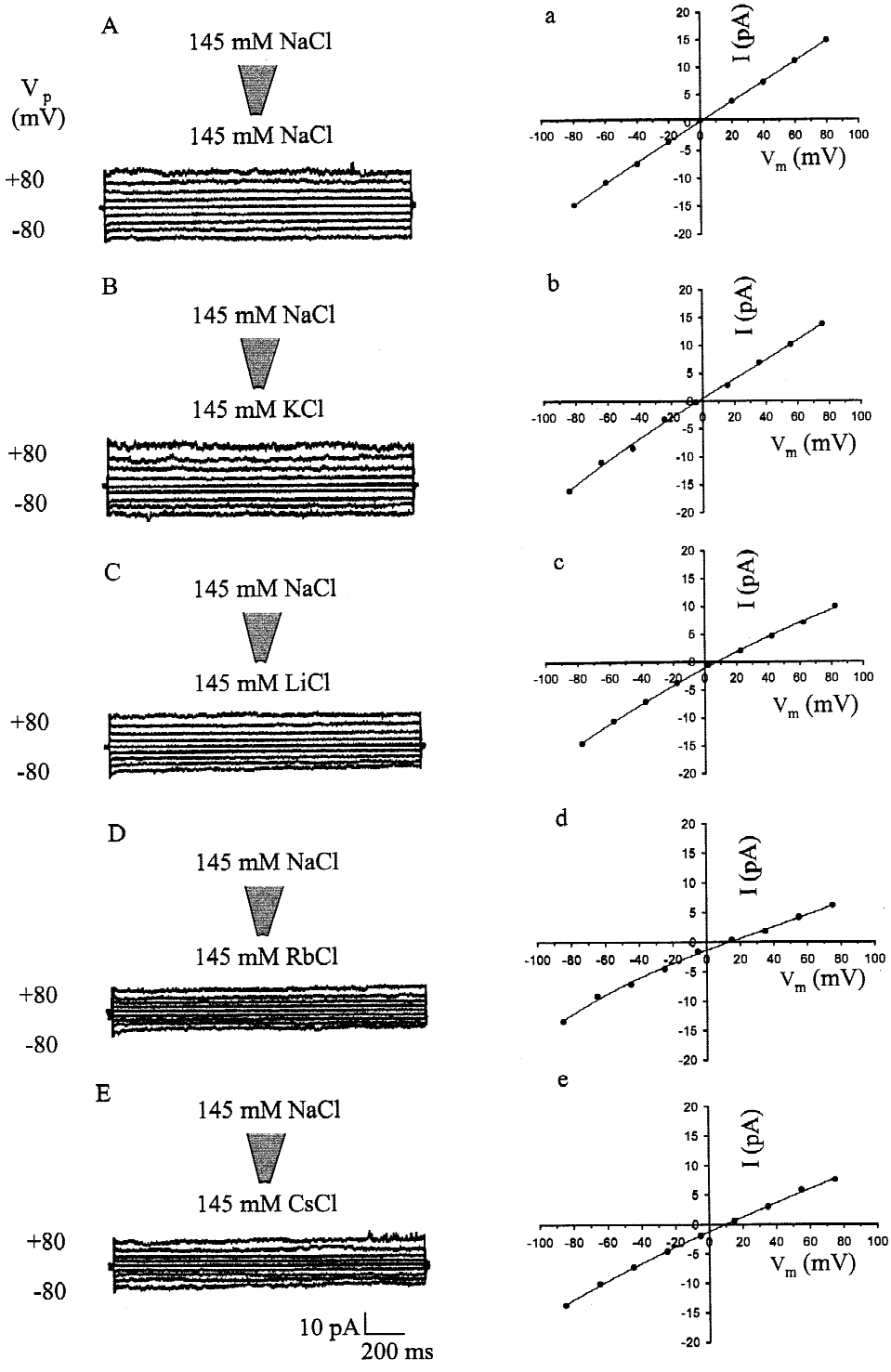

Fig. 6. Macroscopic cAMP-activated currents in different monovalent alkali cation solutions in one inside-out patch from HEK293 cells. (*A–E*) are the representative currents elicited by 500 μM cAMP in response to 1.5 sec voltage pulses (V_P) from −80 to +80 mV in 20-mV steps. The internal membrane surface was perfused with the same concentration of NaCl, KCl, LiCl, RbCl and CsCl solutions (145 mM) and the extracellular NaCl (145 mM) solution was kept constant. The holding potential was 0 mV and background current traces in the absence of cAMP have been subtracted. (*a–e*) are corresponding current-voltage (*I–V*) relations for the adjacent traces. Continuous lines represent the fit of the data points with a quadratic polynomial. The corresponding E_{rev} values (corrected V_m) for this patch were about −1 mV for NaCl, −1.5 mV for KCl, +7.5 mV for LiCl, +14 mV for RbCl and + 10.5 mV for CsCl.

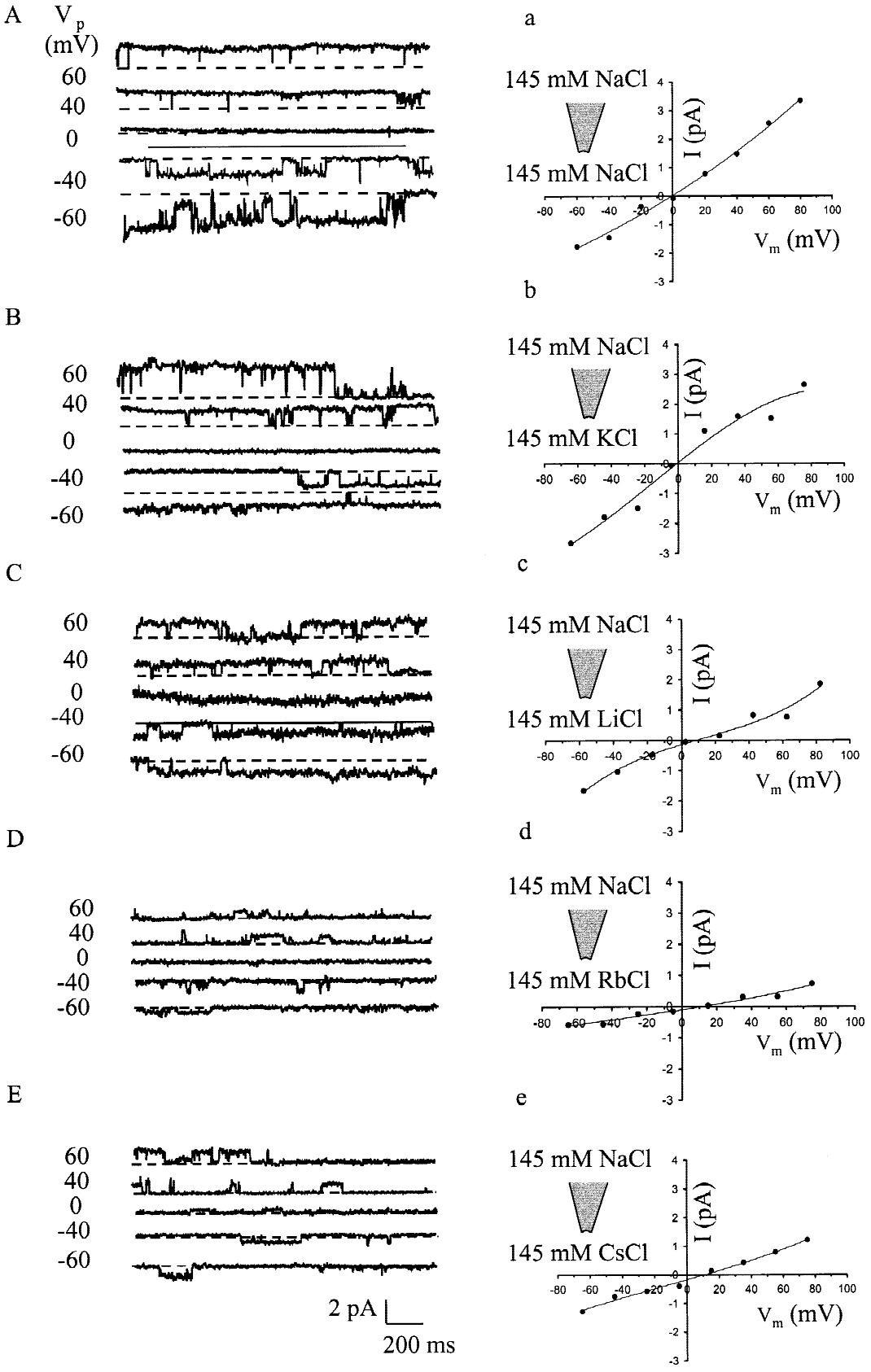

Fig. 7. Cation selectivity of rOCNC1 channels to different monovalent alkali cations measured using single-channel records. (*A–E*) are the representative single-channel currents at several holding potentials (V_P) in one inside-out patch from the HEK293 cells, when the internal membrane was perfused with the same concentration of NaCl, KCl, LiCl, RbCl and CsCl solutions (145 mM). Currents were activated by 500 mM cAMP and the extracellular Na^+ in the pipette was kept the same (145 mM) throughout the experiments. (*a–e*) are *I–V* curves of the single-channel currents shown in (*A–E*), which were obtained by plotting corresponding peak single-channel currents (*I*) against corrected membrane voltage (V_m). Continuous lines represent the fit of the data points with a quadratic polynomial. The corresponding E_{rev} values (measured as V_m) for this patch were about −0.5 mV for NaCl, −1 mV for KCl, +9 mV for LiCl, +12 mV for RbCl and +11 mV for CsCl.

Table 1. Selectivity of rOCNC1 channels for monovalent alkali and organic cations

Test Cations	*n*	ΔE_{rev} (mV)	$[X^+]_i$ (mM)	$[Tris^+]_i$ (mM)	P_X/P_{Na}	P_X/P_{Na} (corrected)	g_X/g_{Na} (+80mV)	g_X/g_{Na} (-80mV)
Li^+	5	7.2 ± 2.2	145	8	0.78	0.74	0.65	0.75
K^+	6	1.6 ± 1.5	145	7	0.98	0.94	0.92	1.20
Na^+	7	0.2 ± 0.3	145	8	1.03	1.00	1.00	1.00
Rb^+	6	14.9 ± 2.0	145	6	0.58	0.55	0.25	0.27
Cs^+	5	12.8 ± 1.6	145	7	0.63	0.59	0.42	0.58
NH_4^+	5	−8.6 ± 2.4	145	12	1.46	1.40	1.07	1.09
$OHNH_3^+$	4	−4.5 ± 0.7	65	43	2.77	2.31	—	—
*$Tris^+$	5	8.3 ± 2.5	145	10	0.70	0.70	0.42	0.43
TEA^+	4	35.2 ± 2.0	145	24	0.26	0.15	0.28	0.69
$Choline^+$	5	17.8 ± 3.2	145	11	0.52	0.47	0.29	0.75

* $[Tris^+]_i$ refers to the concentration of $Tris^+$ used for titrating the corresponding perfused test cation solution to pH 7.4; the ΔE_{rev} values have been corrected for liquid junction potentials; *n* represents the number of experiments used for the average; P_X/P_{Na} is the permeability ratios of test cations relative to Na^+ and P_X/P_{Na} (corrected) is the final value after the correction for $Tris^+$ permeability.

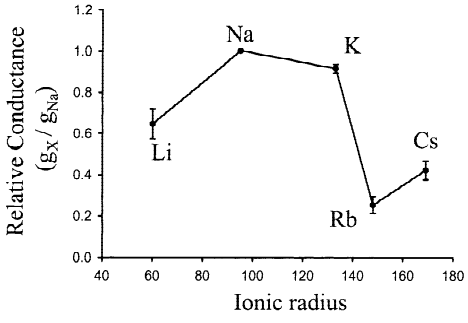

Fig. 8. The relationship between conductance ratios of alkali cations relative to Na^+ in cAMP-activated rOCNC1 channels and ionic radius of each tested ion. The data points were all obtained from one patch. The membrane potential was +80 mV, under which conditions the outward currents might be expected to be mainly carried by the test cation present at the cytoplasmic side of the membrane.

The mean values of E_{rev} in the different solutions, corrected for junction potentials and obtained from single channel current recordings were (e.g., Fig. 9*a–e*): −8.6 ± 2.4 mV for NH_4^+ ($n = 5$), −4.5 ± 0.7 mV for $OHNH_3^+$ ($n = 4$), +8.3 ± 2.5 for $Tris^+$ ($n = 5$), +17.8 ± 3.2 for $choline^+$ ($n = 5$) and +35.2 ± 2.0 for TEA^+ ($n = 4$). The permeability ratios for each cation relative to Na^+, calculated from these E_{rev} values and corrected for $Tris^+$ permeability, were: P_{OHNH3} (2.3) > P_{NH4} (1.4) > P_{Na} (1) > P_{Tris} (0.7) > $P_{Choline}$ (0.5) > P_{TEA} (0.2). These results clearly show that cAMP-gated rOCNC1 channels are more permeable to NH_4^+ and $OHNH_3^+$ than to Na^+ ions, which corresponds well with the properties of the native rat olfactory CNG channels (Balasubramanian et al., 1995). Among all the test organic cations, TEA^+ was the least permeant with small currents at both positive and negative membrane potentials. Figure 10 shows the relationship between the relative permeability of the test organic cations and their molecular weight. The results indicate that the permeability of rOCNC1 channels to organic cations is predominantly determined by the size (molecular weight) of these ions.

In addition to ionic permeabilities, the relative chord conductance ratios in the presence of different organic cations were also measured. Relative conductances at both +80 and −80 mV were calculated by normalizing the measured single-channel conductances in test organic cation solutions to their values in symmetrical Na^+ solutions at the same potential (*see* Table 1). At a membrane potential of +80 mV, the outward currents, predominantly carried by the test ions, gave the following relative chord conductances: g_{NH4} (1.07) > g_{Na} (1) > g_{Tris} (0.42) > $g_{Choline}$ (0.29) > g_{TEA} (0.28). The conductance of hydroxylamine was not included, because of its very different concentration from the other organic cations.

In summary, the permeability sequence of all the test organic cations in rOCNC1 channels was $P_{OHNH3} > P_{NH4} > P_{Na} > P_{Tris} > P_{Choline} > P_{TEA}$, which agrees well with the sequence for native rat CNG channels (Balasubramanian et al., 1995). Because of the finite permeability of TEA, it seems likely that the minimum pore diameter of the channels should be at least 6.5 × 6.5 Å, as suggested by the molecular size of the largest permeant cation (Dwyer, Adams & Hille, 1980).

Discussion

In this present study, we have analyzed the selectivity of cAMP-activated recombinant rOCNC1 channels expressed in HEK 293 cells. The permeability sequence of these channels for monovalent alkali metal ions relative to Na^+ was P_{Na} (1) ≥ P_K (0.97) > P_{Li} (0.77) > P_{Cs} (0.62) ≥ P_{Rb} (0.57). The relative permeability sequences of a variety of test organic cations, again relative to sodium, were P_{NH3OH} (1.88) > P_{NH4} (1.08) > P_{Na} (1) > P_{Tris} (0.66) > $P_{Choline}$ (0.46) > P_{TEA} (0.19). Thus our data demonstrate that α-homomeric rOCNC1 channels have relatively large pores that discriminate poorly amongst alkali cations, particularly between the physiologically

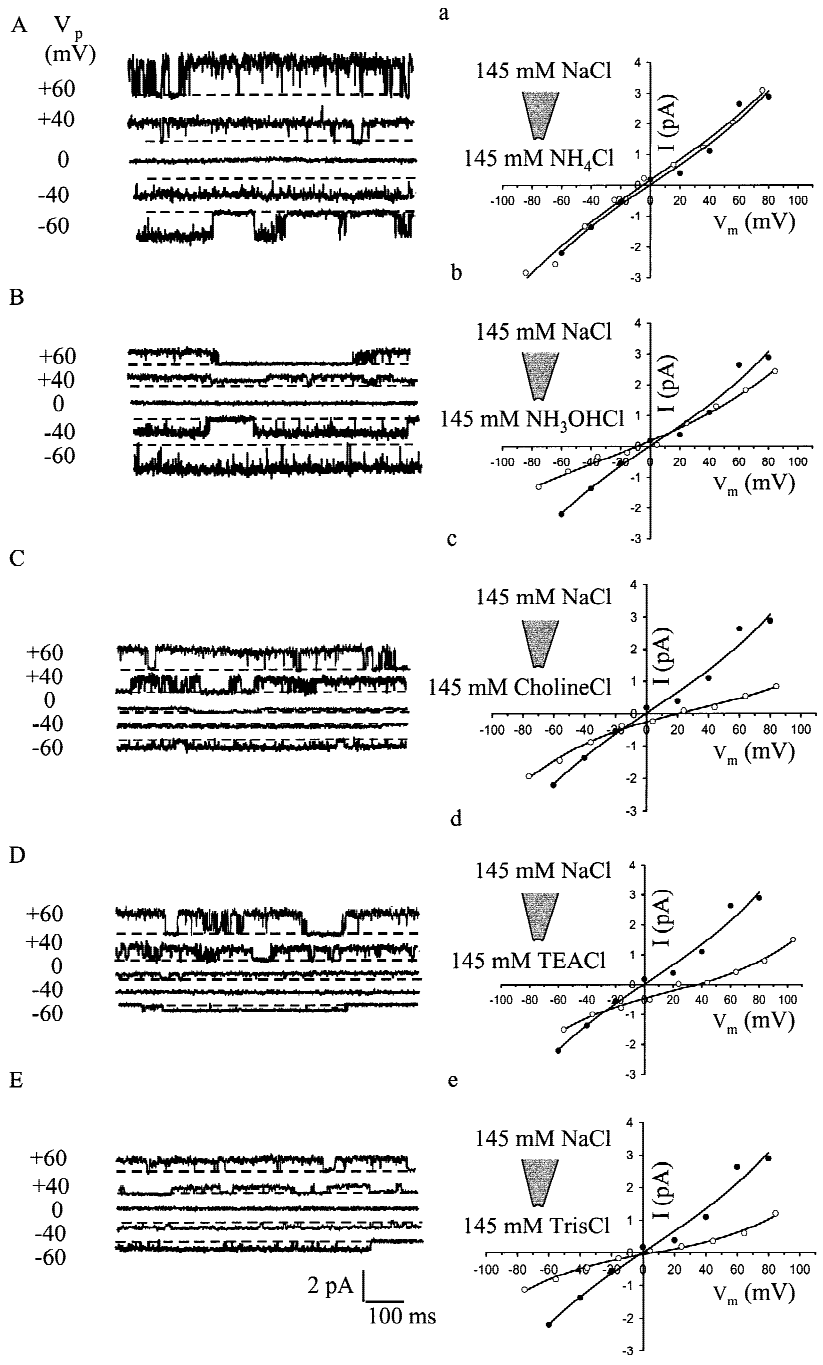

Fig. 9. The permeability of cAMP-activated rOCNC1 channels to organic cations in one inside-out patch of HEK293 cells. (*A–E*) are the representative cAMP-activated single-channel current traces at several holding potentials (measured as V_P), when Na^+ ions were replaced by NH_4^+, $OHNH_3^+$, choline$^+$, TEA^+ and $Tris^+$ at the cytoplasmic side. Currents were activated by 500 μM cAMP and 1.5-sec voltage pulses, from −80 to +80 mV in steps of 10 mV. The dashed lines indicate the current levels of the closed channels. (*a–e*) are the corresponding *I–V* relations of the single-channel current traces shown in *A–E*, which were obtained by plotting the averaged single-channel current, *I* (pA), against the membrane potential, V_m (mV), for the patch from which the parts of the traces are shown in this figure. Both the *I–V* curves in symmetrical Na^+ solutions (filled circles), and responses in solutions with individual test organic cations (open circles), are shown together. The continuous lines represent quadratic polynomial fits to the data points. The values of E_{rev} (measured as V_m) in each solution for this patch were: −9 mV for NH_4^+, −5 mV for $OHNH_3^+$, 7 mV for $Tris^+$, 20 mV for choline$^+$, and 37 mV for TEA^+.

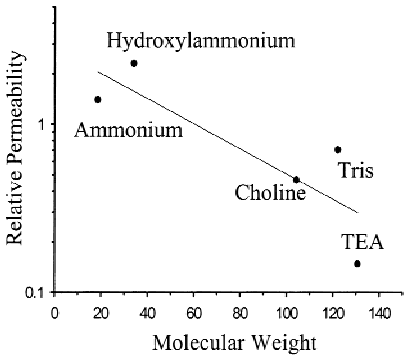

Fig. 10. The relationship between the permeabilities of test organic cations relative to Na^+ (on a log scale) and the molecular weight of the ions in recombinant rOCNC1 channels. The results have been corrected for the permeability of $Tris^+$. The continuous line represents a first-order linear regression fit to the data points. The trend of the data indicates that the permeability of monovalent organic cations through these channels becomes smaller with increasing size of the ion.

important Na^+ and K^+ ions, with their relative permeability (P_K/P_{Na}) in the range of 0.9–1.0. Li^+ has a permeability smaller than that of Na^+ and K^+, but larger than the permeability of Cs^+ or Rb^+. These results are in accordance with data obtained from native CNG channels in other species which do not greatly discriminate between alkali cations (Hodgkin, McLaughton & Nunn, 1985; Nakamura & Gold, 1987; Bruch & Teeter, 1990; Dhallan et al., 1990; Kurahashi, 1990; Frings et al., 1992; Zufall & Firestein, 1993). More specifically, with the exception of the relative permeabilities of Rb^+ and Cs^+ (whose values are quite similar to each other), the permeability sequence and relative permeability ratios of the monovalent cations agree closely with the results obtained from native CNG channels from rat ORNs (Frings et al., 1992; Balasubramanian et al., 1995). This suggests that the permeation properties of the native rat ORN CNG channel is determined primarily by the OCNC1 subunit and that inclusion of other subunits (such as the β-subunits) into the channel complex does not alter permeation to a significant degree. Furthermore, there is also excellent agreement between the data in the present study and that obtained for the CNG channel from native rat ORNs (Balasubramanian et al., 1995) as far as the organic cation permeability sequence is concerned.

Eisenman formulated a model of ion channel permeation based on the difference in the energies of ion hydration and of the electrostatic interaction with a binding site (*see* review in Eisenman & Horn, 1983). The underlying assumption in comparing permeability sequence with such a permeation model is that the permeability is dominated by the partition coefficient or ion concentration within the channel and the mobility or rate constant for movement within the channel (e.g., Barry & Gage, 1984). The permeability sequence obtained in the present study approximates an alkali cation sequence with permeation dominated by energies associated with electrostatic interactions with the binding site(s), i.e., a fairly high-field-strength sequence (≈ sequence IX). In contrast, the relatively nonselective LGICs display a permeability sequence dominated by hydration energies (e.g., Adams, Dwyer & Hille, 1980; Keramidas et al., 2000). On the basis of a lack of anomalous mole fraction behaviour with Li^+ and K^+ as the permeant cations, Frings et al. (1992) concluded that the native rat ORN CNG channel displays only single ion occupancy, suggesting that this high field strength site may reside at a single locus within the pore, although other evidence is more consistent with multiple binding sites (Balasubramanian et al., 1997). In addition, other pairs of ions may be better placed to reveal anomalous mole fraction effects.

The size of the narrowest region of the pore can be roughly estimated from the molecular weight of the largest permeant cations from space-filling models (Dwyer et al., 1980; Picco & Menini, 1993). The present results suggest a minimum pore diameter for homomeric rOCNC1 channels of 6.5 × 6.5 Å. This is of similar size to the native rat olfactory CNG channel (Balasubramanian et al., 1995) and the ligand-activated nicotinic acetylcholine receptor (nAChR) channel at the endplate (Dwyer et al., 1980), but significantly larger than the pore of the squid axon voltage dependent Na^+ (3.0 × 5.0 Å; Hille, 1971) and K^+ channels (3.0 Å diameter; Hille, 1973) and also markedly larger than the retinal rod CNG channel (3.8 × 5.0 Å; Picco & Menini, 1993). It will be interesting to determine why the pore size of the rOCNC1 channels is significantly larger than that of the retinal rod cGMP-activated channels in tiger salamander (Picco & Menini, 1993). Although the fairly high-field-strength sequence indicates that the interactions between the monovalent cation and the binding sites in the pore play a critical role in determining the permeability, the large pore of rOCNC1 channels probably allows the small ions to retain part of their hydration shell so that the magnitude of the selectivity sequence is not so great. Hence, these channels, which belong to the same superfamily as the voltage-gated ion channels, are less discriminative between monovalent alkali cations than are Na^+ and K^+ channels (Hille, 1971, 1973) and can even allow the permeation of quite large methylated cations.

Both permeability and conductance sequences can effectively measure selectivity, but often, or even usually, provide different sequences reflecting the fact that conductance and permeability are sensitive in slightly different ways to the partition coefficient of the ion (or its concentration within the channel) and its mobility or the rate of movement through the channel. In addition, the conductance sequences from macroscopic data are subject to difficulties in interpretation if the permeating ion

somehow affects channel open time. However, in agreement with previous studies on permeation in native rod CNG channels (Sesti et al., 1994), the single channel open probability was not markedly affected by the nature of the permeating ion, for both the alkali and organic cations. Somewhat surprisingly, although similar to the situation in native rat ORN CNG channels (Balasubramanian et al., 1995), the conductance sequence for both the alkali and organic cations was the same as the permeability sequence.

Another interesting and unusual property of these channels, possibly related to the similarity between conductance and permeability sequence discussed above, was that, in the presence of different monovalent cations at the cytoplasmic membrane side of inside-out patches, the values for g_X/g_{Na} of the inward currents also changed in different test solutions, in spite of the expectation (*see* e.g., Barry & Gage, 1984, for ACh channels) that inward currents would mainly be carried by Na^+ ions moving from the pipette to the bath solution. However, similar results have been reported with similar changes in inside test solutions for the inward macroscopic currents of CNG channels obtained in native rat olfactory ORNs (Balasubramanian et al., 1995) and the inward Na^+ conductances in cGMP-activated channels in retinal rods of the tiger salamander (Picco & Menini, 1993). In accord with such results, it has also been observed in native CNG channels in the presence of asymmetrical salt concentration gradients that the conductances tend to reflect the average ion concentrations in both solutions, irrespective of the current direction (Balasubramanian et al., 1997). It will be very informative to explore the precise mechanism of this phenomenon in the light of site-directed mutagenesis experiments.

The results in this paper should prove to be useful as a basis for further understanding the mechanism of ion permeability of the rOCNC1 channel at the molecular level and for elucidating the relationship between the molecular structure and the physiological function of this channel. Extending the approach used for this paper, in combination with site-directed mutagenesis experiments, should thus enable a determination of the role of critical amino acids in elucidating the mechanism of ion selectivity and permeation through these channels.

X.O. Zhu acknowledges the support of the 'Foundation Post-Doctoral Research Award' from University of New South Wales Postgraduate Medical School. We also acknowledge the support of the Australian Research Council, the National Health and Medical Research Council of Australia and the Garnett Passe and Rodney Williams Memorial Foundation.

References

Adams, D.J., Dwyer, T.M., Hille, B. 1980. The permeability of endplate channels to monovalent and divalent metal cations. *J. Gen. Physiol.* **75:**493–510

Balasubramanian, S., Lynch, J.W., Barry, P.H. 1995. The permeation of organic cations through cAMP-gated channels in mammalian olfactory receptor neurons. *J. Membrane Biol.* **146:**177–191

Balasubramanian, S., Lynch, J.W., Barry, P.H. 1996. Calcium-dependent modulation of the agonist affinity of the mammalian olfactory cyclic nucleotide-gated channel by calmodulin and a novel endogenous factor. *J. Membrane Biol.* **152:**13–23

Balasubramanian, S., Lynch, J.W., Barry, P.H. 1997. Concentration dependence of sodium permeation and sodium ion interactions in the cyclic AMP-gated channels of mammalian olfactory receptor neurons. *J. Membrane Biol.* **159:**41–52

Barry, P.H. 1994. JPCalc, a software package for calculating liquid junction potential corrections in patch-clamp, intracellular, epithelial and bilayer measurements and for correcting liquid junction potential measurements. *J. Neurosci. Meth.* **51:**107–116

Barry, P.H., Gage, P.W. 1984. Ionic selectivity of channels at the end plate. *Curr. Top. Membr. Transp.* **21:**1–51

Bönigk, W., Bradley, J., Müller, F., Sesti, F., Boekhoff, I., Ronnett, G.V., Kaupp, U.B., Frings, S. 1999. The native rat olfactory cyclic nucleotide-gated channel is composed of three distinct subunits. *J. Neurosci.* **19:**5332–5347

Bradley, J., Li, J., Davidson, N., Lester, H.A., Zinn, K. 1994. Heteromeric olfactory cyclic nucleotide-gated channels: A subunit that confers increased sensitivity to cAMP. *Proc. Natl. Acad. Sci. USA* **91:**8890–8894

Bruch, K.C., Teeter, J.H. 1990. Cyclic AMP links amino acid chemoreceptors to ion channels in olfactory cilia. *Chemical Senses* **15:**419–430

Chen, C., Okayama, H. 1987. High efficiency expression of mammalian cells by plasmid DNA. *Mol. Cell Biol.* **7:**2745–2751

Dhallan, R.S., Yau, K-W., Schrader, K.A., Reed, R.R. 1990. Primary structure and functional expression of a cyclic nucleotide-activated channel from olfactory neurons. *Nature* **347:**184–187

Dwyer, T.M., Adams, D.J., Hille, B. 1980. The permeability of the endplate channel to organic cations in frog muscle. *J. Gen. Physiol.* **75:**469–492

Eisenman, G., Horn, R. 1983. Ionic selectivity revisited: the role of kinetic and equilibrium processes in ion permeation through channels. *J. Membrane Biol.* **76:**197–225

Eismann, E., Bönigk, W., Kaupp, U.B. 1993. Structural features of cyclic nucleotide-gated channels. *Cell Physiol. Biochem.* **3:**332–351

Eismann, E., Müller, F., Heinemann, S.H., Kaupp, U.B. 1994. A single negative charge within the pore region of a cGMP-gated channel controls rectification, Ca^{2+} blockage and ionic selectivity. *Proc. Natl. Acad. Sci. USA* **91:**1109–1113

Fesenko, E.E., Kolesnikov, S.S., Lyubarsky, A.L. 1985. Induction by cyclic GMP of cationic conductance in plasma membrane of retinal rod outer segment. *Nature* **313:**310–313

Frings, S., Lynch, J.W., Lindemann, B. 1992. Properties of cyclic nucleotide-gated channels mediating olfactory transduction. *J. Gen. Physiol.* **100:**45–67

Gerstner, A., Zong, X., Hofmann, F., Biel, M. 2000. Molecular cloning and functional characterization of a new modulatory cyclic nucleotide-gated channel subunit from mouse retina. *J. Neurosci.* **20:**1324–1332

Getchell, T.V. 1977. Analysis of intracellular recordings from salamander olfactory epithelium. *Brain Res.* **123:**275–286

Goulding, E.H., Ngai, J., Kramer, R.H., Colicos, S., Axel, R., Siegelbaum, S.A., Chess, A. 1992. Molecular cloning and single-channel properties of the cyclic nucleotide-gated channel from catfish olfactory neurons. *Neuron* **8:**45–58

Hamill, O.P., Marty, A., Neher, E., Sakmann, B., Sigworth, F.J. 1981. Improved patch clamp techniques for high resolution current re-

cording from cells and cell-free membrane-patches. *Pfluegers Arch.* **391:**85–100

Heginbotham, L., Abramson, T., MacKinnon, R. 1992. A functional connection between the pores of distantly related ion channels as revealed by mutant K^+ channels. *Science* **258:**1152–1155

Hille, B. 1971. The permeability of the sodium channel to organic cations in myelinated nerve. *J. Gen. Physiol.* **58:**599–619

Hille, B. 1973. Potassium channels in myelinated nerve: Selective permeability to small cations. *J. Gen. Physiol.* **61:**669–686

Hille, B. 1975. Ionic selectivity of Na and K channels of nerve membranes. *In: Membranes-A series of Advances, vol. 3. Lipid Bilayers and Biological Membranes: Dynamic Properties,* G. Eisenman, editor. pp. 255–323. Marcel Dekker, New York

Hille, B. 1992. Ionic Channels of Excitable Membranes. Second edition. Sinauer Associates, Sunderland, MA

Hodgkin, A.L., McLaughton, P.A., Nunn, B.J. 1985. The ionic selectivity and calcium dependence of the light-sensitive pathway in toad rods. *J. Physiol.* **358:**447–468

Kaupp, B.U., Niidome, T., Tanabe, T., Terada, S., Bönigk, W., Suhmer, W., Cook, N., Kangawa, K., Matsuo, H., Hirose, T., Numa, S. 1989. Primary structure and functional expression from complementary DNA of the rod photoreceptor cyclic GMP-gated channel. *Nature* **342:**762–766

Kaupp, U.B. 1995. Family of cyclic nucleotide gated ion channels. *Curr. Opin. Neurobiol.* **5:**434–442

Keramidas, A., Moorhouse, A.J., French, C.R., Schofield, P.R., Barry, P.H. 2000. M2 pore mutations convert the glycine receptor channel from being anion- to cation-selective. *Biophys. J.* **78:**247–259

Kleene, S.J. 1993. Origin of the chloride current in olfactory transduction. *Neuron* **11:**123–132

Kramer, R.H., Siegelbaum, S.A. 1992. Intracellular Ca^{2+} regulates the sensitivity of cyclic nucleotide-gated channels in olfactory receptor neurons. *Neuron* **9:**897–906

Kurahashi, T., Shibuya, T. 1989. Membrane responses and permeability changes to odorants in the solitary olfactory receptor cells of newt. *Zoological Science* **6:**19–30

Kurahashi, T. 1990. The response induced by intracellular cyclic AMP in isolated olfactory receptor cells of the newt. *J. Physiol.* **430:**355–371

Lancet, D., Ben-Arie, N. 1993. Olfactory receptors. *Current Biol.* **3:**668–674

Li, J., Lester, H.A. 1999. Single channel kinetics of the rat olfactory cyclic nucleotide-gated channel expressed in *Xenopus* oocytes. *Mol. Pharmacol.* **55:**883–893

Lowe, G., Gold, G.H. 1993. Nonlinear amplification by calcium-dependent chloride channels in olfactory receptor cells. *Nature* **366:**283–286

Ludwig, J., Margalit, T. Eismann, E., Lancet, D., Kaupp, U.B. 1990. Primary structure of cAMP-gated channel from bovine olfactory epithelium. *FEBS Lett.* **270:**24–29

McKay, D.B., Steitz, T.A. 1981. Structure of catabolite gene activator protein at 2.9 Å resolution suggests binding to left-handed B-DNA. *Nature* **290:**744–749

Nakamura, T., Gold, G.H. 1987. A cyclic nucleotide-gated conductance in olfactory receptor cilia. *Nature* **325:**442–444

Ng, B., Barry, P.H. 1995. The measurement of ionic conductivities and mobilities of certain less common organic ions needed for junction potential corrections in electrophysiology. *J. Neurosci. Methods* **56:**37–41

Picco, C., Menini A. 1993. The permeability of the cGMP-activated channel to organic cations in retinal rods of the tiger salamander. *J. Physiol.* **460:**741–758

Robinson, R.A., Stokes, R.H. 1965. Electrolyte Solutions. 2nd Ed. Butterworths, London

Root, M.J., MacKinnon, R. 1993. Identification of an external divalent cation-binding site in the pore of a cGMP-activated channel. *Neuron* **11:**459–466

Sautter, A., Zong, X., Hofmann, F., Biel, M. 1998. An isoform of the rod photoreceptor cyclic nucleotide-gated channel β subunit expressed in olfactory neurons. *Proc. Natl. Acad. Sci. USA* **95:**4696–4701

Sesti, F., Straforini, M., Lamb, T.D., Torre, V. 1994. Gating, selectivity and blockage of single channels activated by cyclic GMP in retinal rods of the tiger salamander. *J. Physiol.* **474:**203–222

Shabb, J.B., Corbin, J.D. 1992. Cyclic nucleotide-binding domains in proteins having diverse functions. *J. Biol. Chem.* **267:**5723–5726

Weyand, I., Godde, M., Frings, S., Weiner, J., Müller, F., Altenhofen, W., Hatt, H., Kaupp, U.B. 1994. Cloning and functional expression of a cyclic-nucleotide-gated channel from mammalian sperm. *Nature* **368:**859–863

Zagotta, W.N. 1996. Molecular mechanisms of cyclic nucleotide-gated channels. *J. Bioenerg. Biomembr.* **28:**269–278

Zimmerman, A.L., Baylor, D.A. 1992. Cation interactions within the cyclic GMP-activated channel of retinal rods from the tiger salamander. *J. Physiol.* **449:**759–783

Zufall, F., Firestein, S., Shepherd, G.M. 1991. Analysis of single cyclic nucleotide-gated channels in olfactory receptor cells. *J. Neurosci.* **11:**3573–3580

Zufall, F., Firestein, S. 1993. Divalent cations block the cyclic nucleotide-gated channel of olfactory receptor neurons. *J. Neurophysiol.* **69:**1758–1768

Zufall, F., Firestein, S., Shepherd, G.M. 1994. Cyclic nucleotide-gated ion channels and sensory transduction in olfactory receptor neurons. *Ann. Rev. Biophys. Biomol. Struct.* **23:**577–607